C.P. No. 721

C.P. No. 721

MINISTRY OF AVIATION

AERONAUTICAL RESEARCH COUNCIL

CURRENT PAPERS

Calculation of the Turbulent Boundary Layer in the Nozzle of an Intermittent Axisymmetric Hypersonic Wind Tunnel

By

N.B. Wood

LONDON: HER MAJESTY'S STATIONERY OFFICE

1964

PRICE 5s. 6d. NET

Calculation of the Turbulent Boundary Layer in the Nozzle of an Intermittent Axisymmetric Hypersonic Wind Tunnel

- By -
N. B. Wood

September, 1963

SUMMARY

An approximate method of calculating the turbulent boundary layer in a conical nozzle with isothermal wall is described. The momentum integral technique is used together with a skin-friction coefficient which is assumed to depend on the Reynolds number based on the momentum thickness. Following an analysis by Spence of the experimental data of Lobb, Winkler and Persh, a 1/9 power velocity profile is assumed for the boundary layer and the effect of the transverse curvature of the wall is taken into account. Calculations related to the conditions in the R.A.R.D.E. No.3 Hypersonic Gun Tunnel are presented and the results are compared with experimental pitot-survey data.

Notation

a	speed of sound
c_f	skin-friction coefficient
H	boundary-layer form parameter, δ_*/θ
H_i	value of H in incompressible flow
H_p	value of H in two-dimensional flow
$\overline{H}$	$\overline{\delta_*/\theta}$
M	Mach number outside boundary layer
n	power of velocity profile, $\frac{u}{u_e} = \left(\frac{\eta}{\Delta}\right)^{1/n}$
p_{o2}/p_{o1}	ratio of stagnation pressures across normal shock
r	radial distance from axis of nozzle
R	radial distance of nozzle wall from axis

R_*/

Replaces A.R.C.25 062

R_* nozzle throat radius

r_{uc} radius of uniform core of flow in nozzle

s distance measured along nozzle wall

T temperature

u longitudinal velocity (without subscript denotes velocity in boundary layer, distance r from axis)

x distance measured along nozzle axis

y co-ordinate normal to nozzle wall

γ ratio of specific heats

δ boundary-layer thickness

δ_* boundary-layer displacement thickness, $\int_0^\delta \left(1 - \frac{\rho u}{\rho_e u_e}\right) dy$

$\overline{\delta}_*$ $\int_0^\delta \frac{r}{R}\left(1 - \frac{\rho u}{\rho_e u_e}\right) dy$

Δ transformed boundary-layer thickness, $\int_0^\delta \frac{\rho}{\rho_m} dy$

η transformed co-ordinate normal to wall, $\int_0^y \frac{\rho}{\rho_m} dy$

θ boundary-layer momentum thickness, $\int_0^\delta \frac{\rho u}{\rho_e u_e}\left(1 - \frac{u}{u_e}\right) dy$

$\overline{\theta}$ $\int_0^\delta \frac{r}{R}\frac{\rho u}{\rho_e u_e}\left(1 - \frac{u}{u_e}\right) dy$

ϕ parameter defined by equation (17)

μ viscosity

ρ density

σ recovery factor, defined by equation (8)

ω angle between axis and wall of nozzle

Subscripts /

Subscripts

e	conditions at outer edge of boundary layer
m	conditions at intermediate temperature, T_m {equation (11)}
o	tunnel stagnation conditions
p	boundary-layer parameters in two-dimensional flow
r	recovery conditions, given by $\frac{T_r}{T_e} = 1 + \frac{\sigma}{2}(\gamma-1)M^2$
tr	parameter transformed according to equation (4)
w	wall conditions

1. Introduction

A characteristic of hypersonic wind-tunnel nozzles is the development of a thick boundary layer along the walls, thus severely restricting the core of uniform flow which is available for testing models. The thick boundary layer is due to the high temperature generated by the deceleration of the boundary-layer flow from hypervelocities, causing the density in the layer to be low. A pitot survey of the working section of the R.A.R.D.E. No.3 Gun Tunnel was made by Bowman (Ref.1) and the object of the calculations presented here was to compare the results from approximate theory with experimental data.

Using the momentum integral equation for axisymmetric boundary-layer flow, Sivells and Payne (Ref.2) calculated the boundary layer in a continuous-running hypersonic wind tunnel in which the walls were adiabatic. In an intermittent wind tunnel with a very short running time (e.g., the hypersonic gun tunnel) the wall temperature does not change appreciably during the run and for this case an isothermal "cold" wall is assumed. An analysis is given here of the turbulent boundary layer on an isothermal wall using a transformation similar to that employed by Sivells and Payne. However, these authors used a skin-friction law in a form which implied that the skin-friction coefficient varied only with x, the longitudinal co-ordinate. Whilst this simplifies the integration of the momentum integral equation, it is more realistic to assume that the skin friction depends on θ, the momentum thickness. Accordingly, the present analysis is made with this assumption.

Associated with the use of the momentum integral equation for the boundary layer is the assumption of a mean velocity profile. Spence (Ref.3) analysed the experimental boundary-layer data of Lobb, Winkler and Persh (Ref.4) which was obtained over a Mach number range of 5 to 8. The velocity profile which resulted from Spence's analysis was a 1/9 power law profile, i.e.,

$$\frac{u}{u_e} = \left(\frac{\eta}{\Delta}\right)^{1/9} \qquad \ldots (1a)$$

η/

$$\eta = \int_0^y \frac{\rho}{\rho m}\, dy , \qquad \Delta = \int_0^\delta \frac{\rho}{\rho m}\, dy . \qquad \ldots (1b)$$

In the absence of any other data the above profile has been assumed for the present calculations.

When the thickness of the boundary layer in axisymmetric flow approaches radius of curvature of the walls the modification of the momentum and displacement effects of the boundary layer must be taken into account and the approach of Michel (Ref.5) has been followed here.

The boundary layer has been assumed turbulent from the start of the flow since the Reynolds numbers are high throughout (of the order 1×10^6/ft at the throat).

2. Analysis

2.1 Formulation and transformation

The von Kármán momentum equation for axisymmetric boundary-layer flow (Refs.2, 5) is

$$\frac{d\bar{\theta}}{ds} + \bar{\theta}\left[\frac{2 - M^2 + \bar{H}}{M\left(1 + \frac{\gamma-1}{2} M^2\right)} \frac{dM}{ds} + \frac{1}{R}\frac{dR}{ds}\right] = \frac{C_f}{2} \qquad \ldots (2)$$

where C_f is the skin-friction coefficient and $\bar{\theta}$, $\bar{H}$ are defined by

$$\bar{\theta} = \int_0^\delta \frac{r}{R}\frac{\rho u}{\rho_e u_e}\left[1 - \frac{u}{u_e}\right] dy \qquad \ldots (2a)$$

$$\bar{H} = \frac{\bar{\delta}_*}{\bar{\theta}} \qquad \ldots (2b)$$

where

$$\bar{\delta}_* = \int_0^\delta \frac{r}{R}\left(1 - \frac{\rho u}{\rho_e u_e}\right) dy . \qquad \ldots (2c)$$

For a conical nozzle with expansion angle 2ω, $ds = dx \sec\omega$ and if ω is small so that $\sec\omega \to 1$, $ds = dx$. Therefore equation (2) may be rewritten

$$\frac{d\bar{\theta}}{dx} + \bar{\theta}\left[\frac{2 - M^2 + \bar{H}}{M\left(1 + \frac{\gamma-1}{2} M^2\right)} \frac{dM}{dx} + \frac{1}{R}\frac{dR}{dx}\right] = \frac{C_f}{2} . \qquad \ldots (3)$$

In/

In order to simplify the coefficient of dM/dx, equation (3) is now transformed as follows

$$\bar{\theta} = \bar{\theta}_{tr}\left[1 + \frac{\gamma-1}{2} M^2\right]^{\frac{\gamma+1}{2(\gamma-1)}} = \bar{\theta}_{tr}\left[\frac{T_o}{T_e}\right]^{\frac{\gamma+1}{2(\gamma-1)}} \quad \ldots (4a)$$

$$\bar{H} = \bar{H}_{tr}\left[1 + \frac{\gamma-1}{2} M^2\right] + \frac{\gamma-1}{2} M^2 \quad \ldots (4b)$$

i.e., $$\bar{H} + 1 = (\bar{H}_{tr} + 1)\frac{T_o}{T_e}$$

and the following equation is obtained

$$\frac{d\bar{\theta}_{tr}}{dx} + \frac{\bar{\theta}_{tr}}{M}\frac{dM}{dx}(2 + \bar{H}_{tr}) + \frac{\bar{\theta}_{tr}}{R}\frac{dR}{dx} = \frac{C_f}{2}\left[\frac{T_e}{T_o}\right]^{\frac{\gamma+1}{2(\gamma-1)}} . \quad \ldots (5)$$

The above transformation is similar to the generalisation of the Stewartson-Illingworth transformation, used by Spence (Ref.6).

2.2 Evaluation of the form parameter, H

In his analysis of the data of Lobb, Winkler and Persh (Ref.4), Spence (Ref.3) found that the quadratic temperature-velocity relationship was a good approximation to the true variation in the boundary layer. Using this relationship the two-dimensional form parameter, H_p is given by

$$H_p + 1 = \frac{T_w}{T_e} H_{i_p} + \frac{T_r}{T_e} . \quad \ldots (6)$$

For an isothermal wall with temperature T_w specified, since $\frac{T_o}{T_e} = 1 + \frac{\gamma-1}{2} M^2$, equation (6) becomes

H_p/

$$H_p = \left[1 + \frac{\gamma-1}{2} M^2\right] \frac{T_w}{T_o} H_{i_p} + \frac{\sigma}{2} (\gamma-1) M^2 \qquad \ldots (7)$$

where σ is the turbulent wall recovery factor defined by

$$\sigma = \frac{T_r - T_e}{T_o - T_e} \qquad \ldots (8)$$

and is observed to be about 0·89 for air.

Dividing by T_o/T_e and using equation (4b), equation (7) transforms, for $\gamma = 1{\cdot}4$, to

$$H_{tr_p} + 1 = \frac{T_w}{T_o} H_{i_p} + \frac{1 + 0{\cdot}178\, M^2}{1 + 0{\cdot}2\, M^2} \; . \qquad \ldots (9)$$

The foregoing relationships apply to two-dimensional boundary layers but it is shown by Michel (Ref.5) that even for quite large values of δ/R, for a turbulent boundary layer, $\bar{H}/H_p$ is within a few per cent of unity. Therefore equations (7) and (9) may be used to evaluate $\bar{H}$ and $\bar{H}_{tr}$ in axisymmetric turbulent boundary layers.

The incompressible form parameter, H_i is given by $H_i = \frac{n+2}{n}$ and for $n = 9$, $H_i = 11/9$.

2.3 Expression for the skin friction

The Blasius turbulent skin-friction coefficient, modified for compressibility, is (Refs.3,6)

$$\frac{\tau_w}{\rho_e u_e^2} = \frac{\rho_m}{\rho_e} \cdot C \cdot \left[\frac{\rho_e u_e \theta_p}{\mu_m}\right]^{-\frac{2}{n+1}}$$

and for a 1/9 power-law profile this becomes

$$\frac{\tau_w}{\rho_e u_e^2} = \frac{C_f}{2} = \frac{T_e}{T_m} \cdot 0{\cdot}0088 \left[\frac{\rho_e u_e \theta_p}{\mu_m}\right]^{-\frac{1}{5}} \qquad \ldots (10)$$

since pressure is constant across the boundary layer, so that $\frac{\rho_m}{\rho_e} = \frac{T_e}{T_m}$.

Once/

Once again this formula is for two-dimensional boundary layers and writing equation (10) in terms of axisymmetric boundary-layer parameters gives

$$\frac{C_f}{2} = 0{\cdot}0088 \frac{T_e}{T_m}\left[\frac{\rho_e u_e \theta}{\mu_m}\right]^{-\frac{1}{5}}\left[\frac{\theta}{\theta_p}\right]^{\frac{1}{5}}$$

$$= 0{\cdot}0088 \frac{T_e}{T_m}\left[\frac{\rho_e u_e \bar{\theta}}{\mu_m}\right]^{-\frac{1}{5}}\left[\frac{\theta}{\theta_p}\right]^{\frac{1}{5}}\left[\frac{\bar{\theta}}{\theta}\right]^{\frac{1}{5}}$$

$$= 0{\cdot}0088 \frac{T_e}{T_m}\left[\frac{\rho_e u_e \bar{\theta}}{\mu_m}\right]^{-\frac{1}{5}}\left[\frac{H_p + 11}{H + 11}\right]^{\frac{1}{5}}\left[1 - \frac{\theta}{2R}\right]^{\frac{1}{5}} \quad \ldots (10a)$$

for a 1/9 power-law velocity profile and small ω. The last two terms in equation (10a) are close to unity and writing it in terms of the transformed momentum thickness leads to

$$\frac{C_f}{2} = 0{\cdot}0088 \frac{T_e}{T_m}\left[\frac{T_e}{T_o}\right]^{\frac{\gamma+1}{10(\gamma-1)}}\left[\frac{\rho_e u_e \bar{\theta}_{tr}}{\mu_m}\right]^{-\frac{1}{5}} . \quad \ldots (10b)$$

2.4 The intermediate temperature, T_m, and calculation of viscosity, μ

The commonly used definition of the intermediate or reference temperature T_m is that due to Eckert (Ref.7) and is

$$T_m = 0{\cdot}5\,(T_w + T_e) + 0{\cdot}22\,(T_r - T_e) . \quad \ldots (11a)$$

For an isothermal wall, T_w is specified and T_m is written in the form

$$\frac{T_m}{T_e} = 0{\cdot}5\,(1 + 0{\cdot}078\,M^2) + 0{\cdot}5\,\frac{T_w}{T_o}\,(1 + 0{\cdot}2\,M^2) \quad \ldots (11b)$$

for air with $\gamma = 1{\cdot}4$, $\sigma = 0{\cdot}89$.

The viscosity, μ, may be calculated from Southerland's law which is, for air, with T in $^{\circ}K$,

μ/

$$\mu = \frac{T^{3/2} \times 3{\cdot}059 \times 10^{-8}}{T + 114} \qquad \ldots (12)$$

measured in slug/ft sec. There is no need to introduce a simpler approximate relation when integrating numerically on an electronic digital computer, as has been done here.

2.5 Integration of the momentum equation

From equations (5) and (10b) the momentum equation may be written

$$\frac{d\bar{\theta}_{tr}}{dx} + \frac{\bar{\theta}_{tr}}{M}\frac{dM}{dx}(2 + H_{tr}) + \frac{\bar{\theta}_{tr}}{R}\frac{dR}{dx} = 0{\cdot}0088\,\frac{T_e}{T_m}\left[\frac{T_e}{T_0}\right]^{\frac{3(\gamma+1)}{5(\gamma-1)}}\left[\frac{\rho_e u_e \bar{\theta}_{tr}}{\mu_m}\right]^{-\frac{1}{5}} . \qquad \ldots (13)$$

If both sides of equation (11) are now multiplied by $\frac{6}{5}\bar{\theta}_{tr}^{\frac{1}{5}}\left[RM^{H_{tr}+2}\right]^{\frac{6}{5}}$, the left-hand side of the equation becomes a perfect differential if $H_{tr} + 2$ can be assumed constant over the interval of integration. Fig.1 shows the variation of $H_{tr} + 2$ with M and demonstrates that this is a reasonable assumption. Therefore equation (11) simplifies to

$$\left[\bar{\theta}_{tr}RM^{H_{tr}+2}\right]^{\frac{6}{5}}\Big|_a^b = \int_a^b 0{\cdot}0106\left[RM^{H_{tr}+2}\right]^{\frac{6}{5}}\frac{T_e}{T_m}\left[\frac{T_e}{T_0}\right]^{\frac{3(\gamma+1)}{5(\gamma-1)}}\left[\frac{\rho_e u_e}{\mu_m}\right]^{-\frac{1}{5}} dx . \qquad \ldots (14)$$

The parameters in the above equation are functions of Mach number M and so it is simpler to integrate w.r.t.M. The one-dimensional theory for the uniform core gives

$$\frac{R - \delta_*}{R_*} = \sqrt{\frac{1}{M}}\left[\frac{1 + \frac{\gamma-1}{2}M^2}{(\gamma+1)/2}\right]^{\frac{\gamma+1}{4(\gamma-1)}} \qquad \ldots (15)$$

from which

$\frac{dR}{dM}$ /

$$\frac{dR}{dM} - \frac{d\delta_*}{dM} = \frac{R_*}{2}\sqrt{\frac{1}{M^3}}\,\frac{(M^2-1)\left(1+\frac{\gamma-1}{2}M^2\right)^{\frac{5-3\gamma}{4(\gamma-1)}}}{\left(\frac{\gamma+1}{2}\right)^{\frac{\gamma+1}{4(\gamma-1)}}} \qquad \ldots (16a)$$

and since $\frac{dR}{d\omega} = \tan\omega \simeq \omega$, equation (16a) becomes

$$dx = \frac{R_*}{2\omega}\sqrt{\frac{1}{M^3}}\,\frac{(M^2-1)\left(1+\frac{\gamma-1}{2}M^2\right)^{\frac{5-3\gamma}{4(\gamma-1)}}}{\left(\frac{\gamma+1}{2}\right)^{\frac{\gamma+1}{4(\gamma-1)}}}\cdot dM + \frac{d\delta_*}{dM}\cdot\frac{dM}{\omega}\cdot \qquad \ldots (16b)$$

Substituting equation (16b) in equation (13) and since

$$(\rho_e u_e)^{-\frac{1}{5}} = (\rho_0 a_0)^{\frac{1}{5}}\,\frac{(1+0{\cdot}2\,M^2)^{\frac{3}{5}}}{M^{\frac{1}{5}}}$$

for $\gamma = 1{\cdot}4$, equation (13) becomes

$$\left[\bar{\theta}_{tr}\,RM^{H_{tr}+2}\right]^{\frac{6}{5}}\Big|_a^b = \phi$$

$$= \frac{0{\cdot}0106\,T_0}{\omega(\rho_0 a_0)^{\frac{1}{5}}}\int_a^b\left[\frac{R_*}{\sqrt{M}}\left(\frac{1+0{\cdot}2\,M^2}{1{\cdot}2}\right)^{\frac{3}{2}}+\delta_*\right]^{\frac{6}{5}}\cdot\frac{M^{(6H_{tr}+11)/5}}{(1+0{\cdot}2\,M^2)^4}\cdot\frac{(\mu_m)^{\frac{1}{5}}}{T_m}\cdot$$

$$\times\left[\frac{R_*}{2}\sqrt{\frac{1}{M^2}}\,\frac{(M^2-1)(1+0{\cdot}2\,M^2)^{\frac{1}{2}}}{(1{\cdot}2)^{\frac{3}{2}}}+\frac{d\delta_*}{dM}\right]dM\,. \qquad \ldots (17)$$

Since the geometry of the conical expansion has been included in equation (17), the equation is only valid for the supersonic region downstream of the throat and so the limits of integration are $a = 1$, $b = M_n$. Using a similar expression applied to the subsonic contraction an estimate may be made of the boundary-layer thickness at the throat.

With/

With equations (11b) and (12) substituted into equation (17), the latter may be integrated numerically to obtain ϕ.

Since δ_* and $\frac{d\delta_*}{dM}$ are not initially known, it is necessary to assume that they are zero initially and then by iteration a true solution can be obtained.

2.6 Calculation of the boundary-layer thicknesses

To obtain $\bar{\theta}$ from ϕ, equation (4a) and (15) are substituted into the left-hand side of equation (17) to give

$$\bar{\theta} = \frac{(1 + 0{\cdot}2\,M^2)^3\,\phi^{\frac{5}{6}}}{RM^{H_{tr}+2}}$$

$$= \frac{(1 + 0{\cdot}2\,M^2)^3\,\phi^{\frac{5}{6}}}{\left[\frac{R_*}{\sqrt{M}}\left\{\frac{1 + 0{\cdot}2\,M^2}{1{\cdot}2}\right\}^{\frac{3}{2}} + \delta_*\right]M^{H_{tr}+2}} \qquad \ldots (18)$$

evaluated at $M = M_n(x)$.

The value of $\bar{\delta}_*$ is given by (under the assumptions made in §2.2)

$$\bar{\delta}_* = H\bar{\theta} = \bar{\theta}\left[\frac{T_w}{T_o}(1 + 0{\cdot}2\,M^2)\,H_i + 0{\cdot}178\,M^2\right]. \qquad \ldots (19)$$

The true momentum and displacement thicknesses, θ and δ_*, are obtained from the expressions (Ref.8)

$$\bar{\theta} = \theta - \frac{\theta^2 \cos\omega}{2R}$$

$$\ldots (20)$$

$$\bar{\delta}_* = \delta_* - \frac{\delta_*^2 \cos\omega}{2R} \quad .$$

It may not be possible to allow for the variation of H_i with pressure gradient in the present application without making wildly speculative assumptions (Ref.6), but for most purposes H_i can be assumed to remain constant (Refs.6,8) and in particular for a 1/9 power velocity profile, $H_i = 11/9$.

From/

From equations (1) and the definitions of the momentum and displacement thicknesses, which are

$$\theta = \int_0^{\delta} \frac{\rho u}{\rho_e u_e}\left(1 - \frac{u}{u_e}\right) dy$$

$$\delta_* = \int_0^{\delta} \left(1 - \frac{\rho u}{\rho_e u_e}\right) dy \qquad \ldots (21)$$

it can be shown that for $\left(\frac{u}{u_e}\right) = \left(\frac{\eta}{\Delta}\right)^{\frac{1}{9}}$, the thickness of the boundary layer δ is

$$\delta = \delta_*\left(1 + \frac{11}{H}\right)$$

$$= \theta\,(H + 11)\,. \qquad \ldots (22)$$

It will be seen from equation (19) that as M becomes large H also becomes large. Thus, at high Mach number δ_* is of the same order as δ whereas θ is a smaller fraction of δ compared with the value at low Mach numbers. This is because the gas in most of the boundary layer is much hotter than in the uniform core and so the density is lower. Thus, in equations (21) the term $\frac{\rho u}{\rho_e u_e}$ is small in comparison with unity across most of the layer.

3. Results

Equation (17) was integrated numerically with the aid of an electronic digital computer AMOS (Ferranti Mark 1*), using a 16 point Gauss quadrature formula, for the conditions in the nozzle of the R.A.R.D.E. 10 inch hypersonic gun tunnel. The tunnel has a conical nozzle with a 4° semi-angle and the Mach number is varied by interchangeable throat inserts. The conditions considered were as follows:

Table 1 /

Table 1

Nozzle Throat Diameter (in.)	Nominal Mach Number	Stagnation Temperature (°K)	Stagnation Pressure (p.s.i.)	T_e
0·599	8	1000	2290	65
0·345	10	1300	2580	57
0·200	13	1400	2490	41

The working gas was air.

Figs.2, 3 and 4 show the calculated inviscid and boundary layer - modified Mach number variation down the nozzle for the three cases. Also included are the measured centre-line Mach numbers (Ref.1). Four iterations were required to obtain the Mach 8 results and seven for the other two. Estimates of the boundary-layer thicknesses at the throat were made and although the displacement thicknesses were very small, they were taken into account in the calculations. It will be observed that the agreement between experiment and calculation is best at the lowest Mach numbers. Figs.5, 6 and 7 show the calculated boundary-layer displacement and total thicknesses and Figs.8, 9 and 10 show the calculated total thicknesses in the working section plotted on the pitot traverse results. It will be seen that it is difficult to decide exactly the position of the edge of the boundary layer from the pitot traverses but it can be seen that the calculated values give a good estimate.

By calculating the area ratios $\left(\frac{\text{survey station}}{\text{throat}}\right)$ necessary to give the measured Mach numbers in the core a mass defect thickness can be calculated which should correspond to the boundary-layer displacement thickness. Since the measured and calculated axial Mach number variations did not exactly correspond, the "measured" displacement thicknesses may be compared with theory either at the same value of x or of M as in Table 2.

Table 2 /

Table 2

Throat Diameter (in.)	M	x (in.)	δ* expt. (in.)	Calculated δ* (in.) at value of M (Col.2)	at value of x (Col.3)
0·599	8·3	70·2	0·74	1·00	0·94
	8·5	73·2	0·72	1·10	1·00
	8·7	76·2	0·66	1·20	1·07
0·345	10·2	72·1	1·04	1·70	1·43
	10·4	75·1	0·99	1·82	1·51
	10·7	78·1	0·95	2·04	1·60
0·200	12·7	73·2	1·12	2·86	1·98
	12·9	76·2	1·22	3·00	2·10
	13·0	79·2	1·31	3·09	2·22

The analysis by Spence of the data of Lobb et al has already been mentioned as the basis of the theory used here. The expression for the form parameter H {equation (6)} has been based on the fact that the quadratic temperature-velocity relationship appeared to hold. However, if the measured value of δ_*/θ from Ref.4 is compared with that calculated from equation (6) there is a strong disagreement as shown in Table 3.

Table 3

Ref.4			Eqn.(6)
M_∞	T_w/T_∞	δ_*/θ	$H = \frac{\delta_*}{\theta}$
4·93	5·42	11·42	10·96
5·75	6·19	12·92	13·45
6·83	6·34	13·92	16·05
7·67	5·94	12·47	17·73
8·18	6·60	11·52	19·97

A/

A further example of the failure of equation (6) at hypersonic Mach numbers is provided by the following comparison of some results from the hypersonic tunnel at R.A.E. Farnborough (Ref.9).

Table 4

Ref.9				Eqn.(6)
Time from Flow Start (sec)	M_∞	T_w/T_∞	δ_*/θ	$H = \frac{\delta_*}{\theta}$
15	8·41	7·86	15·0	22·25
60	8·42	6·75	11·7	20·85

In the light of this any agreement between experiment and theory in the present or any other calculations based on equation (6) must be regarded as fortuitous.

Equation (6) is based on assumptions regarding the incompressible form parameter H_i and the turbulent recovery factor σ (giving the recovery temperature T_r). Both H_i and σ may vary considerably instead of remaining constant as is usually assumed. The difficulty of allowing for the variation of H_i with pressure gradient has already been mentioned. This is because the pressure gradients developed in hypersonic nozzle expansions are far in excess of any encountered in incompressible flow.

If it is assumed that the recovery factor remains at about 0·89 at high Mach numbers, then the parameters H_i and H_{tr} can be calculated from equations (6) and (9) using the experimental values of $H = \delta_*/\theta$ from the N.O.L. and R.A.E. results. It is then evident that H_i and H_{tr} are not constant, as has been assumed. It was noted, however, that the factor $H_i + T_o/T_w$ was approximately constant for all the results considered,

i.e., $$\frac{T_e}{T_w}\left(1 + \frac{\delta_*}{\theta}\right) + \frac{T_o - T_r}{T_w} \simeq \text{const.} = K \text{ (say)} .$$

This leads to the approximate empirical formula

$$H = \frac{T_w}{T_e} K - \frac{T_o - T_r}{T_e} - 1$$

where $$K \simeq 2·4 .$$

A/

A simpler empirical formula was noted by Lee (Ref.10). This was

$$\frac{\delta}{\delta_*} = 2{\cdot}5$$

and in fact the N.O.L. and R.A.E. results are all near this figure, the arithmetical mean being 2·4.

However, it is clearly most unsatisfactory to propose empirical laws of this kind, with no theoretical backing, and it is plain that there is considerable scope for both theoretical and experimental research to improve our knowledge of turbulent boundary layers in hypersonic flow.

4. Conclusions

The turbulent boundary layer in the nozzle of the R.A.R.D.E. 10 in. gun tunnel has been calculated using the momentum equation and an assumed power-law profile based on experimental observations. Good agreement between theory and experiment was obtained for the total boundary-layer thickness but because of discrepancies in the theory this is regarded as fortuitous. There was a definite inconsistency between the experimental and calculated boundary-layer displacement thicknesses.

In order to design high Reynolds number hypersonic wind tunnels with confidence, there is a need for more experimental and theoretical research in turbulent hypersonic boundary layers.

References /

References

No.	Author(s)	Title, etc.
1	J. E. Bowman	Unpublished War Office Memo. 1962.
2	J. C. Sivells and R. G. Payne	A method of calculating turbulent boundary layer growth at hypersonic Mach numbers. AEDC-TR-59-3, March, 1959.
3	D. A. Spence	Velocity and enthalpy distributions in the compressible turbulent boundary layer on a flat plate. Journal of Fluid Mechanics, Vol.8, No.3, 1960.
4	R. K. Lobb, E. M. Winkler and J. Persh	N.O.L. Hypersonic Tunnel No.4. Results VII: Experimental investigation of turbulent boundary layers in hypersonic flow. NavOrd Report 3880, March, 1955,
5	R. Michel	Developpement de la couche limite dans une tuyere hypersonique. AGARD Specialists' Meeting "High temperature aspects of hypersonic flow". Rhode-Saint-Genese, Belgium, April, 1962.
6	D. A. Spence	The growth of compressible turbulent boundary layers on isothermal and adiabatic walls. A.R.C. R.& M.3191. June, 1959.
7	E. R. G. Eckert	Engineering relations for friction and heat transfer in high velocity flow. J. Aero. Sci., Vol.22, No.8, August, 1955.
8	E. C. Maskell	Approximate calculation of the turbulent boundary layer in two-dimensional compressible flow. Unpublished M.O.A. Report.
9	J. F. W. Crane	Private communication.
10	J. D. Lee	Axisymmetric nozzles for hypersonic flows. Ohio State University Research Foundation, TN AlOSU 459-1, 1959.

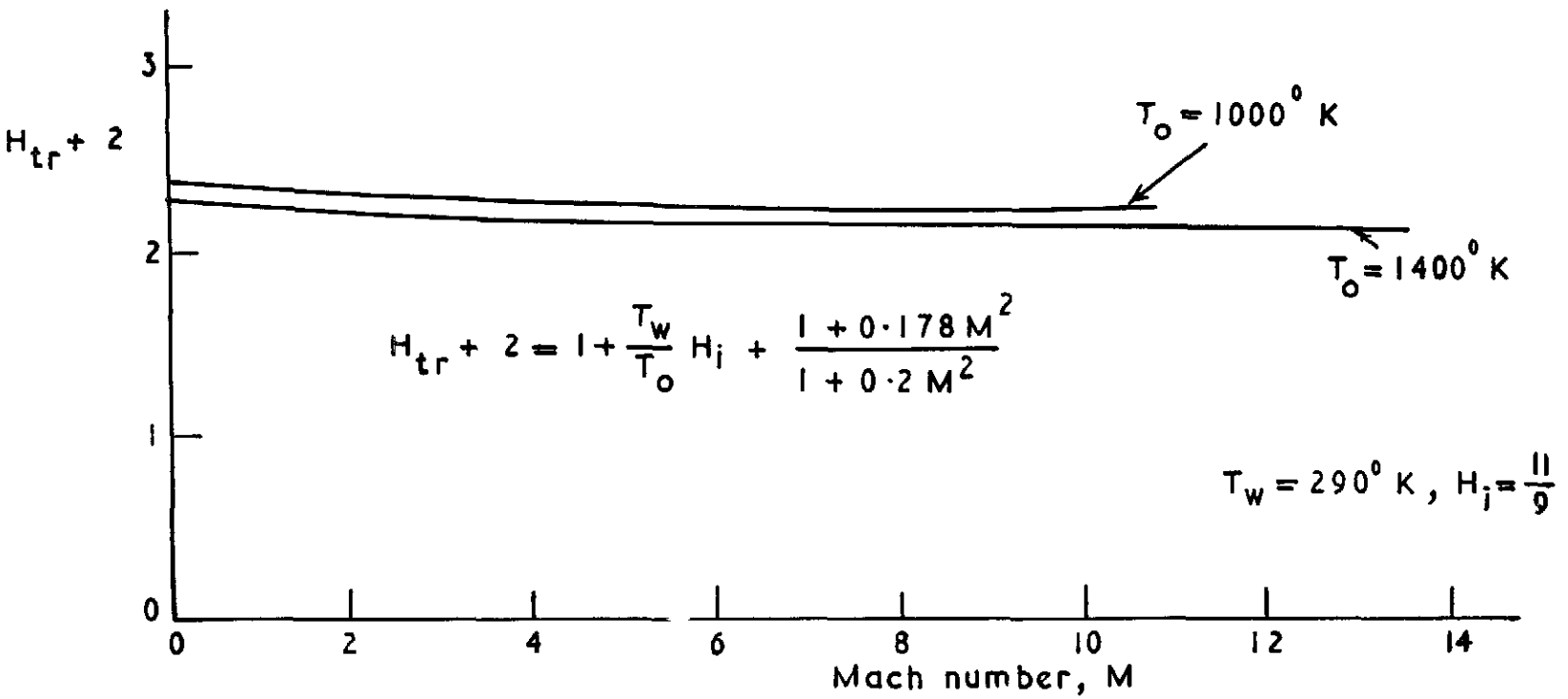

FIG. 1 Variation of $H_{tr}+2$ with Mach number. $\left[\frac{u}{u_e} = \left(\frac{\eta}{\Delta}\right)^{1/9}\right]$

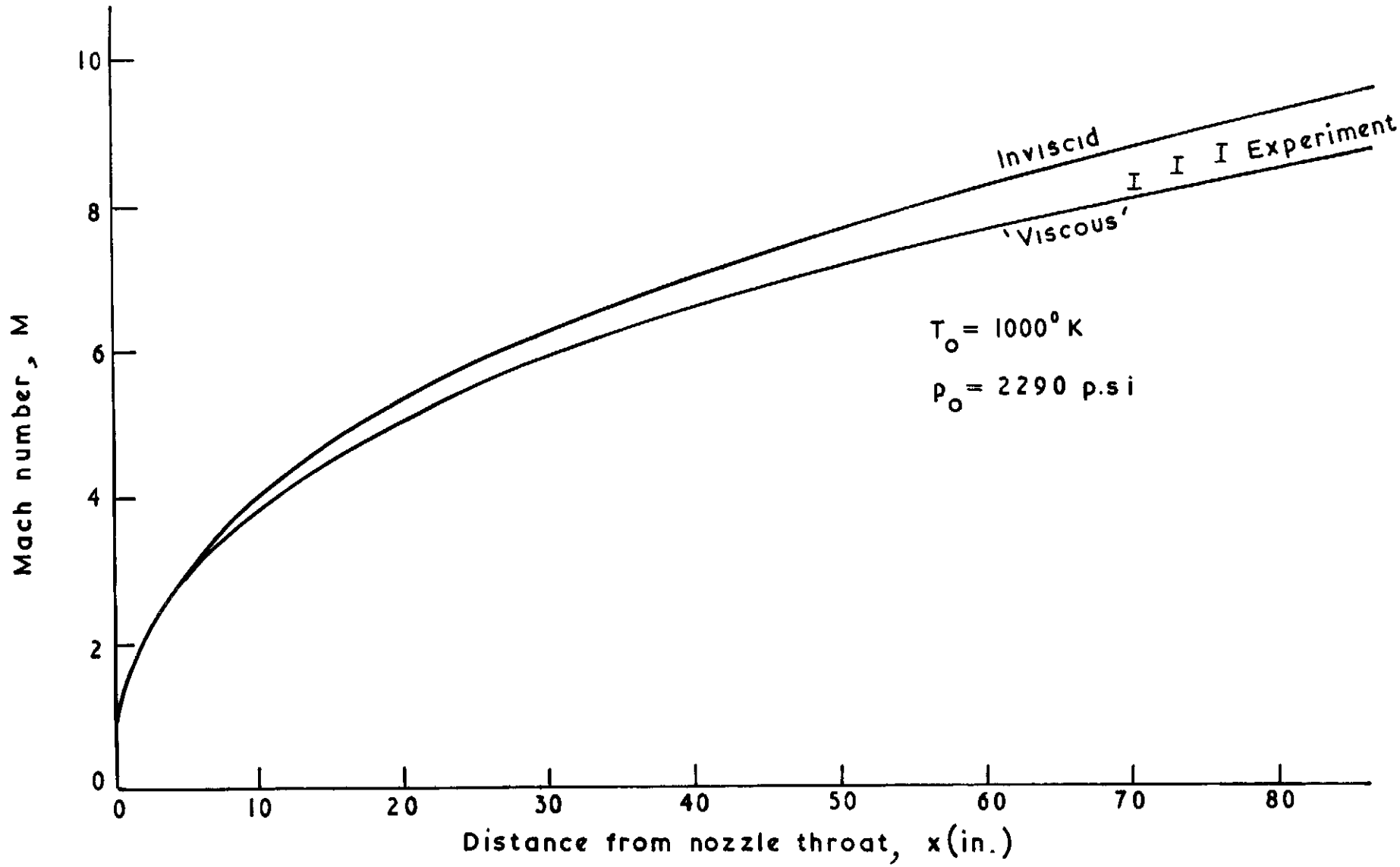

FIG. 2 Axial variation of Mach number in nozzle. ($D_* = 0 \cdot 599''$)

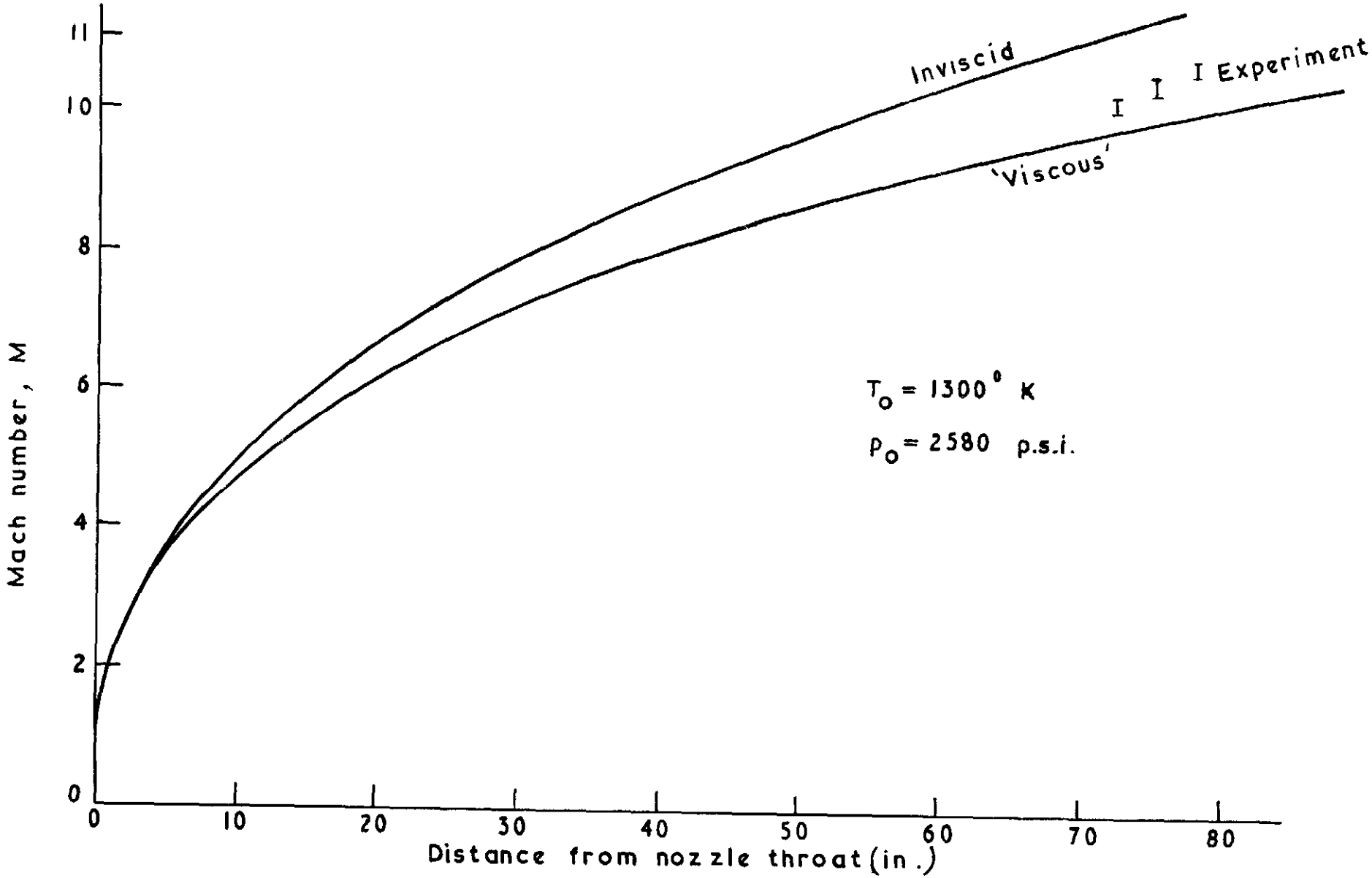

FIG. 3 Axial variation of Mach number in nozzle ($D_* = 0{\cdot}345''$)

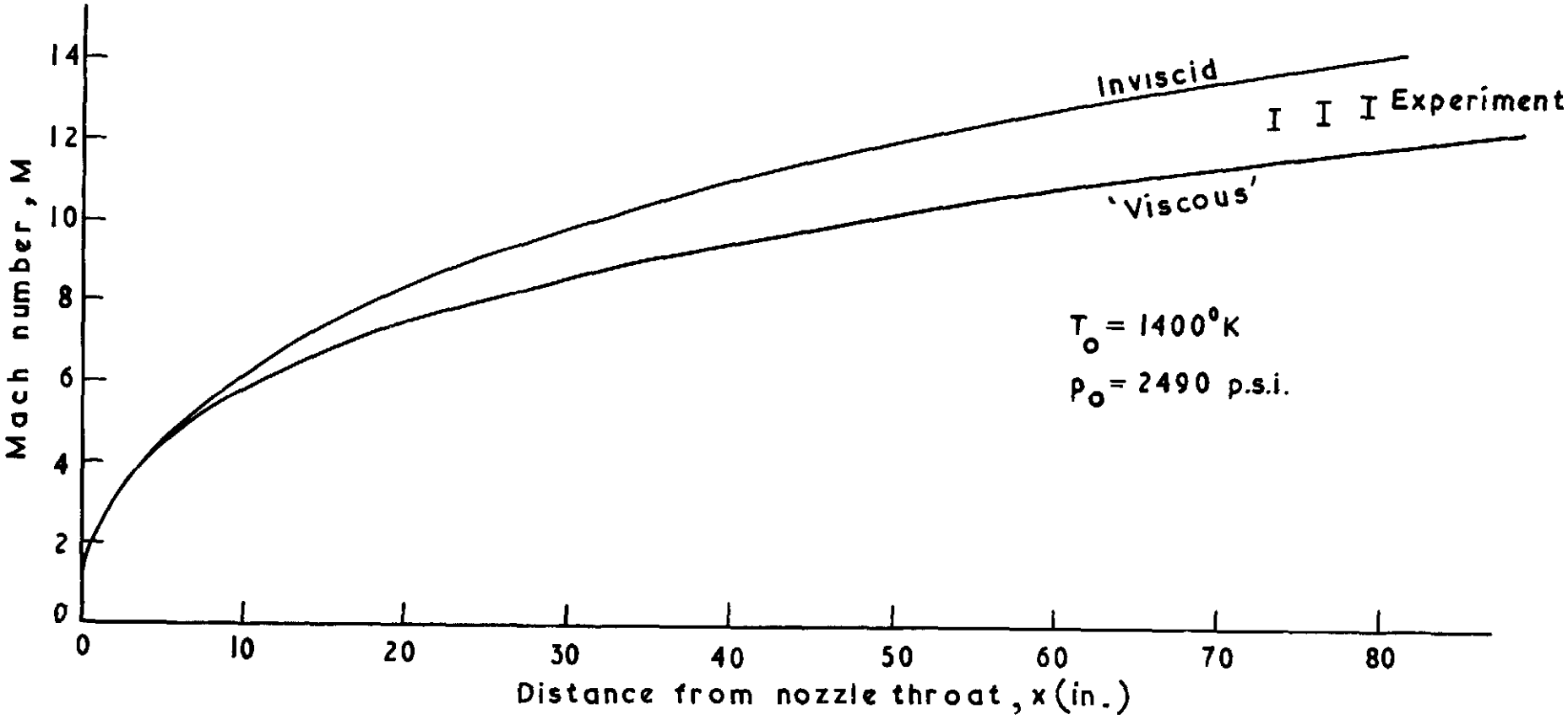

FIG. 4 Axial variation of Mach number in nozzle ($D_* = 0{\cdot}200''$)

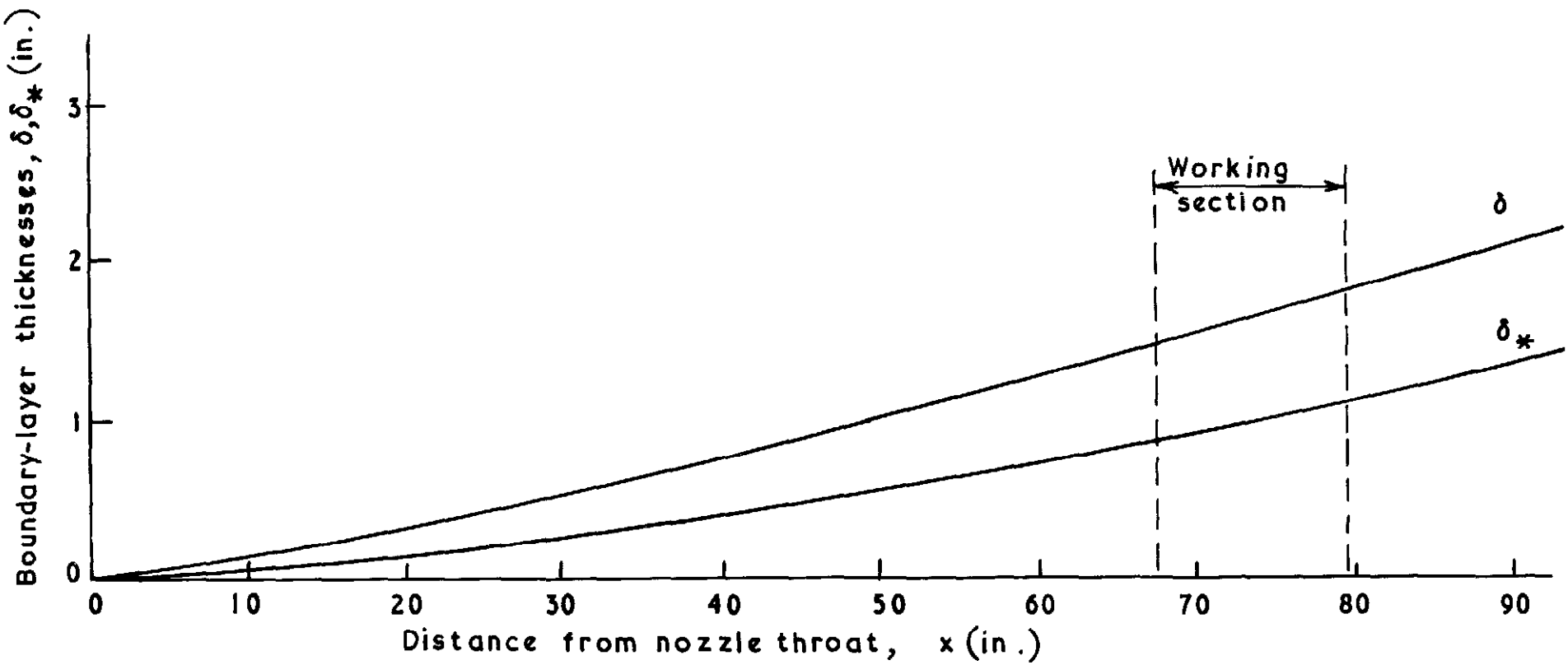

FIG. 5 Calculated boundary-layer growth in Mach 8 nozzle.

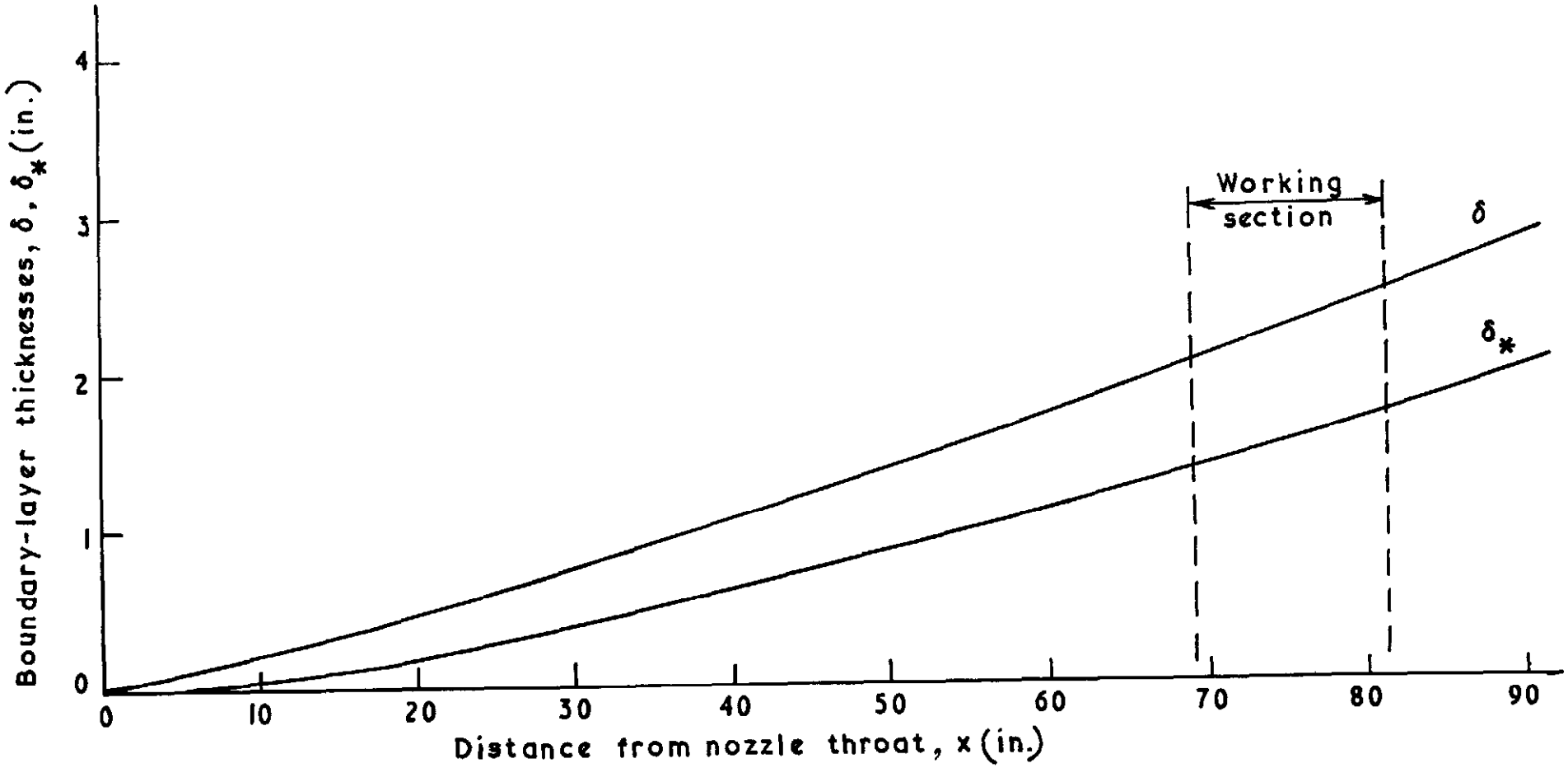

FIG 6 Calculated boundary-layer growth in Mach 10 nozzle.

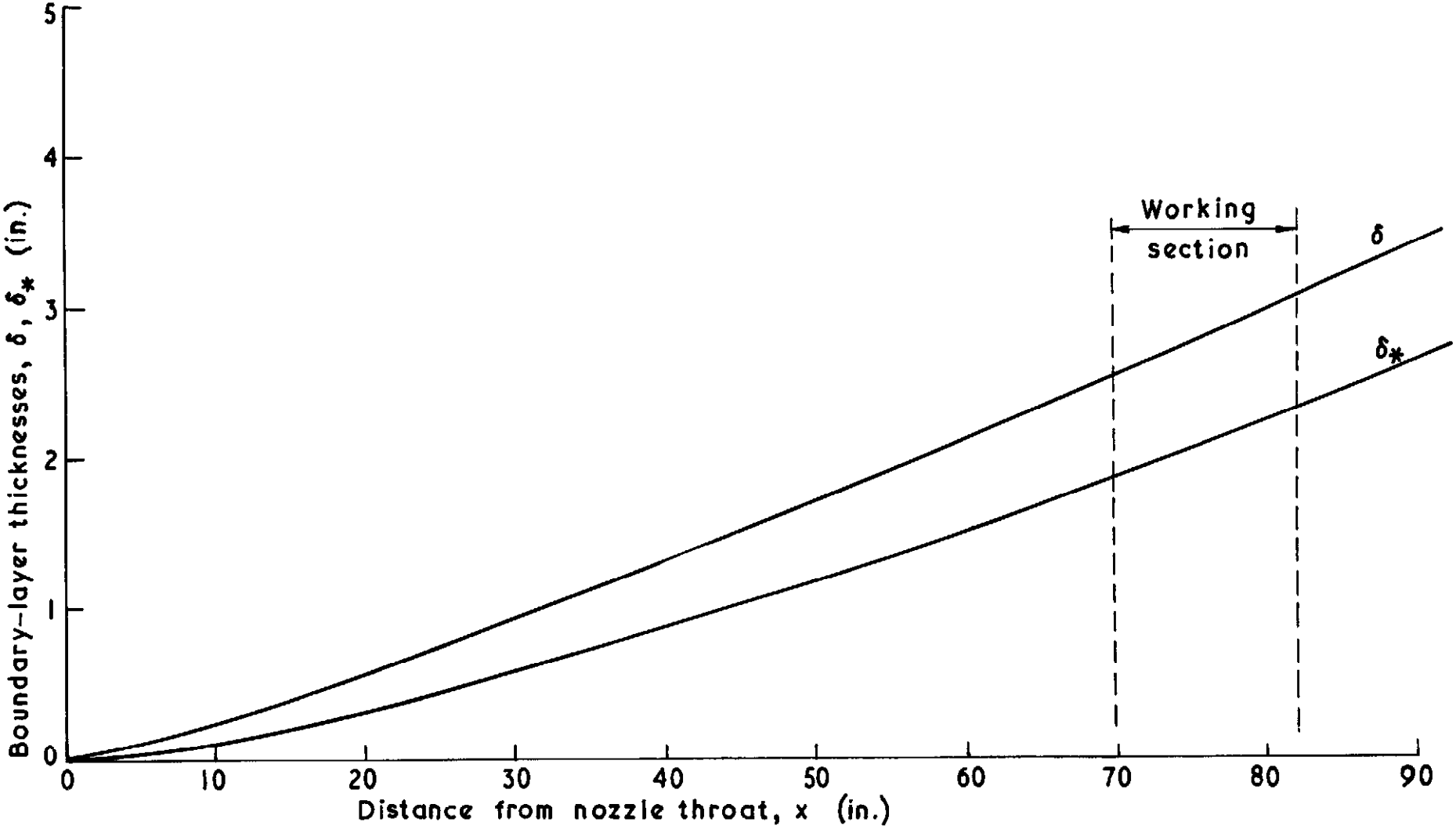

FIG. 7 Calculated boundary-layer growth in Mach 13 nozzle

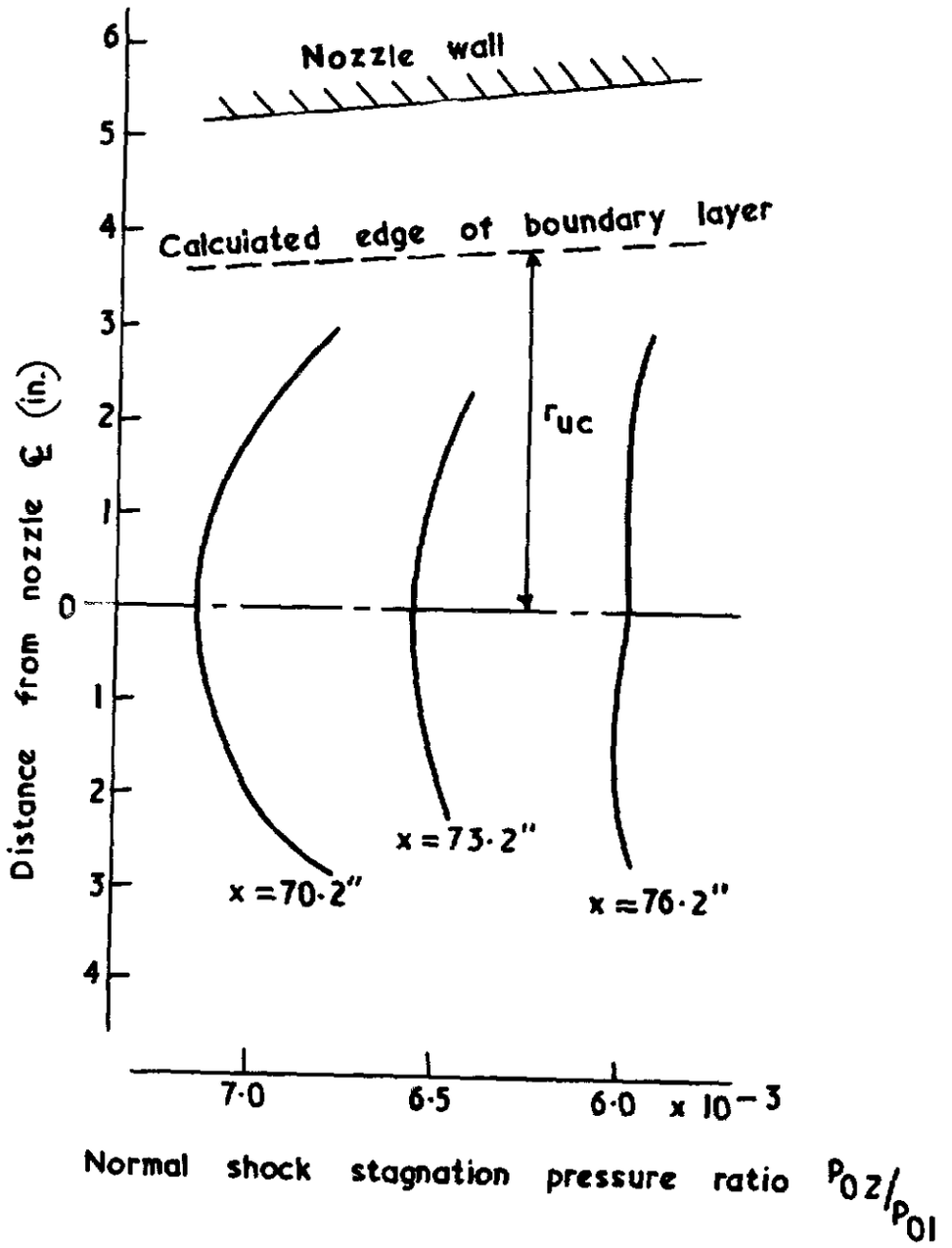

FIG 8. Comparison of calculated uniform core radius (r_{uc}) with experimental pitot traverses. ($D_* = 0.599"$) (Mach 8 throat.)

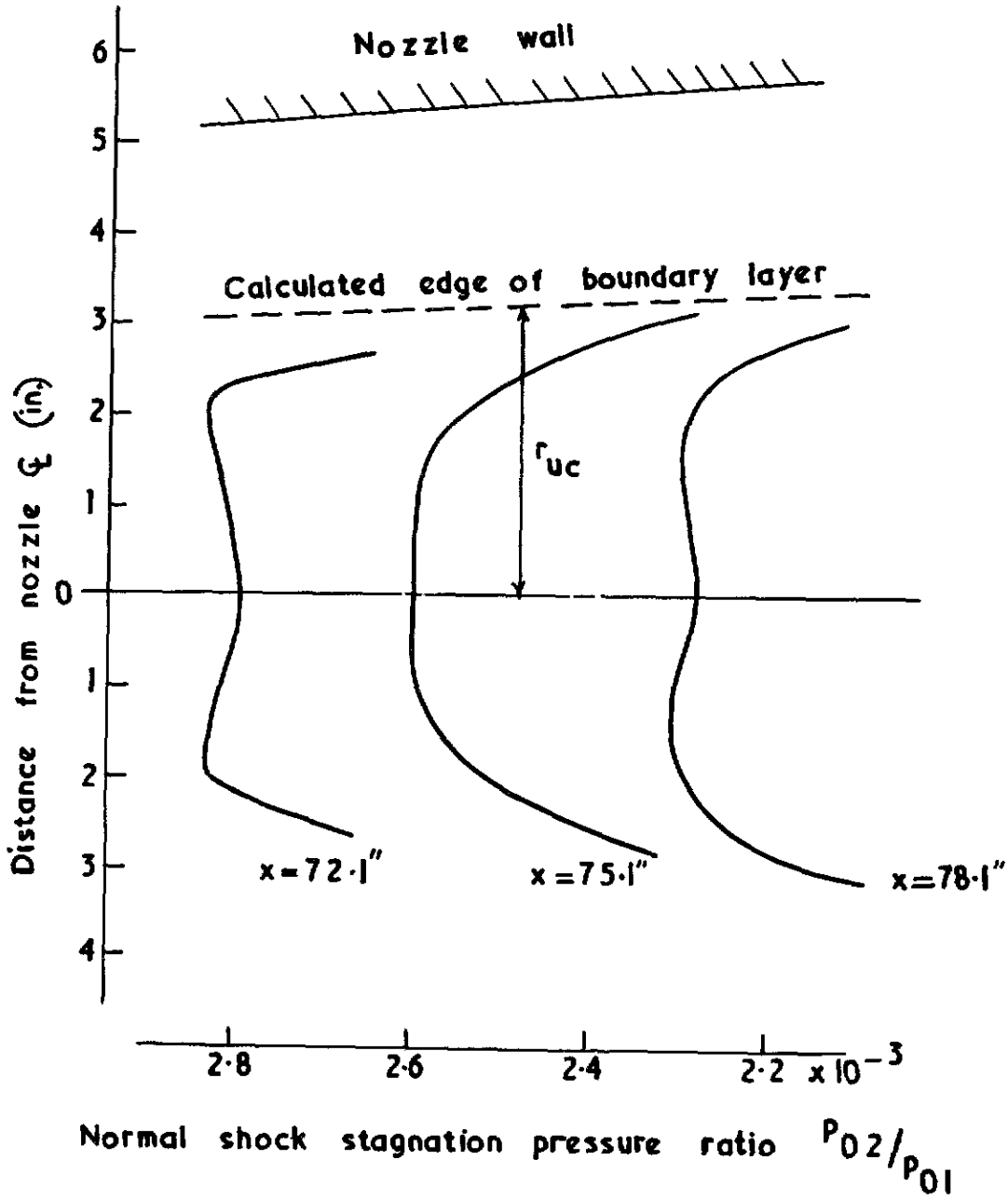

FIG.9 Comparison of calculated uniform core radius (r_{uc}) with experimental pitot traverses. ($D_* = 0{\cdot}345"$) (Mach 10 throat.)

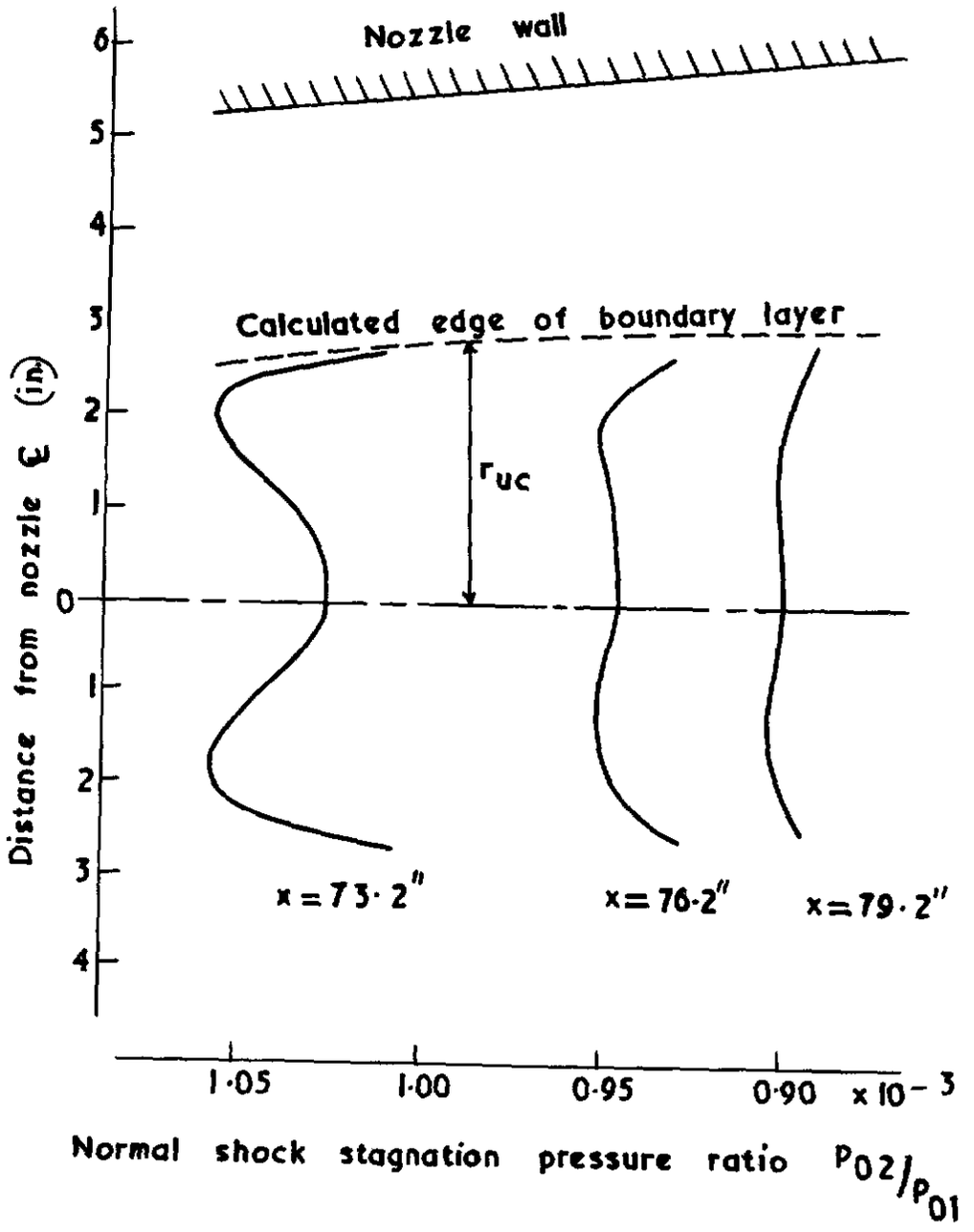

FIG.10 Comparison of calculated uniform core radius (r_{uc}) with experimental pitot traverses. ($D_* = 0.200"$) (Mach 13 throat)

Printed and published by
HER MAJESTY'S STATIONERY OFFICE
To be purchased from
York House, Kingsway, London W C.2
423 Oxford Street, London W 1
13A Castle Street, Edinburgh 2
109 St Mary Street, Cardiff
39 King Street, Manchester 2
50 Fairfax Street, Bristol 1
35 Smallbrook, Ringway, Birmingham 5
80 Chichester Street, Belfast 1
or through any bookseller

Printed in England

S.O. Code No. 23-9015-21